Sorption analysis of composites based on zinc oxide for catalysis and medical materials science

Evgeniya Maraeva [a] *, Dmitriy Radaykin [a], Anton Bobkov [a],
Nikita Permiakov [a], Vasily Matveev [b], Alexander Maximov [a],
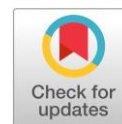Vyacheslav Moshnikov [a]

a: Department of Micro- and Nanoelectronics, Saint-Petersburg Electrotechnical University «LETI», Saint-Petersburg 197022, Russia

b: Petersburg Nuclear Physics Institute named by B.P. Konstantinov, NRC «Kurchatov Institute», Gatchina 188300, Russia

* Corresponding author: jenvmar@mail.ru

This paper belongs to a Regular Issue.

Abstract

Modified structures based on zinc oxide are of special interest in catalysis and medicine. The work discusses the composite structures based on zinc oxide and hydroxyapatite, as well as silver-modified zinc oxide nanostructures obtained by chemical deposition. The obtained materials were studied using a Rigaku SmartLab diffractometric complex and a Sorbi MS sorption analyzer. The specific surface area was studied and the average size of nanoparticles in the samples is determined. The application scope of the considered materials was catalysis and medicine, including the use in bone engineering as bioactive coatings deposited on the surface of a metal bioimplant.

Key findings

● Silver-modified zinc oxide nanostructures and nanocomposites based on zinc oxide and hydroxyapatite were obtained via chemical deposition method.

● The specific surface area was 5–20 m²/g, the nanoparticle sizes were 60–260 nm, depending on the synthesis features.

● The use of silver nanoparticles leads to a decrease in the specific surface area of zinc oxide modified with silver and increases the rate of photocatalytic decomposition.

1. Introduction

Zinc oxide is considered to be one of the most important semiconductor photocatalysts due to its high photosensitivity and good chemical stability [1]. The synthesis of this material can be carried out using the hydrothermal method, the homogeneous precipitation, the sol-gel method and other known methods.

One of the disadvantages of zinc oxide is a wide band gap (3.2–3.3 eV), due to which the material absorbs light only in the near UV region. Unfortunately, metal oxide semiconductors use only 5% of the solar spectrum range [2, 3]. Thus, the efficient use of solar energy remains a challenge in photocatalytic applications of zinc oxide.

The main mechanism of photocatalysis includes the excitation of the ZnO band gap by photons, resulting in the generation of exciton pairs with holes in the valence band and electrons in the conduction band. These charge carriers may recombine, dissipating energy as heat, or may interact with pre-adsorbed electron donors/acceptors on the catalyst surface. Further, donors/acceptors initiate redox reactions with organic pollutants and destroy them. It should be noted that the intensity of the photocatalysis process is affected by the size of the ZnO crystallite. Small particle size leads to a high specific surface area, which improves the ability to absorb photons and increases the probability of adsorption of dye molecules on the surface, and also leads to the suppression of exciton binding [4].

To improve the photocatalytic efficiency of zinc oxide, colloidal quantum dots of semiconductor materials are deposited on its surface, which inject charge carriers upon irradiation in the visible spectral range [5]; plasmonic nanoparticles [6] (including in the form of dendrites [7]) can also be deposited. The other ways are to change the mor-

phology [8] or to change the concentration of intrinsic defects on the surface by special alloying [9]. High-energy electron beams [10], plasma chemistry [11], mechanical activation [12, 13], and other energy effects are used as modifying techniques. A special technological direction is the creation of nanocomposites with desired properties of heterojunctions and energy levels at interfaces [14].

In addition, the LSPR (local surface plasmonic resonance) effect is worth mentioning. This effect occurs as a result of the modification by nanoparticles (NPs) of noble metals (Ag and Au) [15, 16]. LSPR affects the mechanism of charge separation at the metal-semiconductor interface. As a result, an increase in the lifetime of photoinduced electron-hole pairs is observed. Reducing the probability of recombination has a positive effect on the generation of highly active radicals on the catalyst surface. This feature attracts the attention of researchers to the development of plasmonic photocatalysts [17].

Another important area of zinc oxide application – developments in the field of medical materials science – is also associated with heterosystems [18, 19]. In dental applications, the leading positions are occupied by hydroxyapatite (HA) and composite materials based on it. While the properties of hydroxyapatite as a biocompatible material that is an analogue of bone tissue are widely known and have been studied in detail, the problem of bacterial and microbial effects when using such structures in practice remains unresolved. To improve the antibacterial properties of hydroxyapatite, its combinations with zinc and its oxide are used.

Thus, in [20], the results of the studies of the biocompatibility and antibacterial properties of multiphase nanocomposite materials based on HA:ZnO, which were synthesized using calcium nitrate tetrahydrate, ammonium hydrogen phosphate, aqueous ammonia, zinc nitrate hexahydrate, and calcium chloride, are presented. The antimicrobial activity of the samples was assessed on test cultures of gram-negative bacteria (*E. coli*, *P. aeruginosa*) and gram-positive bacteria (*S. aureus* and *S. epidermidis*). Mouse fibroblast cells were used for biocompatibility testing and cytotoxicity evaluation. It was shown that the synthesized nanocomposite material has a multiphase nanoscale architecture, where ZnO nanocrystals are represented by two lattices: cubic and hexagonal. The studied composite demonstrates a high antibacterial activity due to the inclusion of ZnO particles in the hydroxyapatite powder.

In [21], composites based on polycaprolactone, hydroxyapatite and zinc oxide were studied at various mass fractions of zinc oxide. The antimicrobial activity of the obtained scaffolds was shown with a gradual increase in antimicrobial efficiency with increasing ZnO concentration (optimally at 15 and 30% ZnO in the composition). Such composites may be ideal for achieving optimal biocompatibility (cell proliferation, biomineralization and antimicrobial capacity) and mechanical stability, making them a promising biomaterial for bone tissue regeneration.

In [22], HA/ZnO nanorod composite coatings were fabricated on Si substrates. ZnO nanorods were first grown on a substrate by a hydrothermal method, and then a solution of Ca and P precursors was deposited on the surface by centrifugation and fired to form composite coatings of the HA/ZnO nanorods. The wettability of the surface of such a coating can be controlled by ultraviolet treatment, changing from rather hydrophobic to hydrophilic. Such coatings showed a different adsorption capacity of the protein for both the ZnO nanorod coating and the HA coating. The desired ability to release Zn ions was also observed. Such coatings can potentially be applied as bioactive coatings to the surface of a metal bioimplant.

The aim of [23] was to create a platform with optimal physicochemical properties and photocatalytic activity for the delivery of the standard chemotherapeutic drug doxorubicin. In [24], a highly sensitive and selective sensor with a carbon-modified electrode based on the "hydroxyapatite-ZnO-Pd" composite was made for the simultaneous determination of arbutin and vitamin C.

Let us consider in more detail the reason for the increased interest in zinc oxide as an antibacterial component of composite structures. The work [25] describes the antibacterial properties of zinc and its oxide. Zinc is one of the most widespread mineral elements in hard tissues; this element plays various physiological roles in the immune system, and is also involved in cell division and growth. Zinc oxide (ZnO) has unique optical-electrical and chemical properties. ZnO promotes bone tissue regeneration, and also has antimicrobial activity with enhanced mechanical properties. ZnO nanoparticles have three characteristic mechanisms of antimicrobial action, mainly through the generation of reactive oxygen species, attack on the nucleus and protein, and destruction of the cell wall. These modes of action differ from the mechanism of microbial resistance formation, i.e. isolation, drug modification, target modification, and enzyme deactivation. Therefore, zinc oxide nanoparticles are considered to be the most suitable nanoantibiotics for bacteria resistant to other antibiotics.

It is important to note that the antimicrobial activity of ZnO depends on the particle size, which in turn regulates the internalization of Zn^{2+}.

At present, sorption methods of analysis, including the method of thermal nitrogen desorption (NTD), are widely used to characterize the porous structure parameters of nanomaterials for a wide range of functional purposes. NTD belongs to the group of non-destructive techniques that provide express analysis of such parameters of nanomaterials as specific surface area, average particle size, mesopore size distribution, and presence or absence of micropores in the system [26].

The aim of this work was to obtain composite structures based on zinc oxide and hydroxyapatite, as well as zinc oxide with silver additives, to study their phase composition, specific surface area and nanoparticle size.

2. Experimental

In this work, the samples of zinc oxide obtained by chemical deposition with the addition of silver nanoparticles, as well as a series of samples of "zinc oxide – hydroxyapatite" (HA:ZnO) composites were chosen as the objects under study.

For the tasks of photocatalysis, zinc oxide powders were synthesized with and without the participation of a surface-active agent (SAA) sodium dodecyl sulfate.

2.1. Synthesis without SAA

Zinc acetate was dissolved in an aqueous medium with a volume of 25 ml to obtain the aqueous solution of 0.1 M. Then a sodium hydroxide solution of 0.2 M was prepared (25 ml). The solution with zinc acetate was stirred at 950 rpm, and the solution with NaOH was poured into it. As a result, the solution became turbid. Next, the final solution with a volume of 50 ml was heated to 100 °C and kept at this temperature for 1 hour. The finished product (precipitate) was separated from the solution by centrifugation and used in photocatalysis.

2.2. Synthesis with SAA

The technique is similar to the previous one, the differences are as follows: together with a portion of zinc acetate, a portion of surfactant 0.01 M was added; after centrifugation, the powder was washed 7 times before being examined in photocatalysis.

Using the sodium hydroxide precipitation method, the following samples were synthesized:

1) ZnO without the addition of SAA and Ag NPs (pure zinc oxide);

2) ZnO without SAA, but with the addition of Ag NPs;

3) ZnO with the addition of SAA, without Ag NPs;

4) ZnO with the addition of SAA and Ag NPs:

5) ZnO with the addition of SAA and Ag NPs with agglomeration of silver nanoparticles.

The difference between samples 4 and 5 is a result of heating the solution with zinc acetate and surfactant during the addition of Ag NPs. Upon heating and adding the particles, the color of the solution changed from yellow to red, and the nanoparticles underwent agglomeration. In order to exclude this process in the future, the nanoparticles were added to the solution at room temperature.

The silver nanoparticles were synthesized by the citrate method using silver nitrate ($AgNO_3$); sodium citrate ($Na_3C_6H_5O_7$) and deionized water as a solvent.

2.3. Preparation of HA:ZnO composites

The initial powders of hydroxyapatite for the composites were obtained by chemical deposition with the use of microwave radiation. The details of the synthesis are reported in [27]. To obtain zinc oxide, the technology described in [28] was taken, where to synthesize zinc oxide 0.5 ml of 0.5 M zinc nitrate solution ($Zn(NO_3)_2 \cdot 6H_2O$) was mixed with 30 ml distilled water containing 0.5 g of cetyl-trimethyl-ammoniumbromide (CTAB), followed by adding 5 ml of NaOH solution. The concentration of the NaOH solution was estimated on the assumption of $[Zn^{2+}]:[OH^-]=1:10$ ratio. The solution was mixed in an ultrasonic bath (100 W), vigorously stirred for 5 minutes and transferred to the thermostat (90 °C) for 2 hours. The products were collected by centrifugation and washed 3 times in distilled water. ZnO powder was then dried at 80 °C and annealed at 350 °C for 20 minutes.

The initial powders of hydroxyapatite and zinc oxide were mechanically mixed and subjected to manual pressing using a mold with a diameter of 7 mm. As a result of pressing, a series of tablets with a height of about 1100 μm was obtained.

2.4. Research methods

The phase composition was studied using a Rigaku SmartLab (Cu Kα) diffractometric complex. The X-ray diffraction patterns were taken in the quasi-parallel beam mode in the angle range $2\theta = 10{-}80°$ with a step $\Delta(2\theta) = 0.02°$.

The sorption characteristics of the composites were studied using a Sorbi MS device (Russia, Novosibirsk). The output signal is a desorption peak, the area of which is proportional to the volume of adsorbed/desorbed gas. To recalculate the peak area into the volume of adsorbed gas, preselected coefficients were used. The calibration coefficients were obtained in the study of standard samples with known specific surface area. In this work, the standard sample with a specific surface area SBET = 106 m^2/g was used to calibrate the device. The data analysis was carried out according to the results of processing the desorption peaks, taking into account the selected calibration coefficients.

As part of the work, a series of adsorption isotherms was studied in the range of relative partial pressures of adsorbate gas (nitrogen) P/P_0 0–20%, the specific surface area of each composite was determined by the standard Brunauer-Emmett-Teller (BET) method, and the average particle size in the sample was estimated. The average particle size was estimated using the data on the specific surface area and density according to the method described in [26].

3. Results and Discussion

Figure S1 shows the X-ray diffraction pattern of the zinc oxide powder used to create the HA:ZnO composites. Figure S2 shows the X-ray diffraction pattern of the HA:ZnO (1:1) composite. When studying the composition of the the HA:ZnO structures, the presence of lines related to the phases HA (ICCD: 01-074-0565), ZnO (ICCD: 01-076-0704) and, in some cases, calcium carbonate $CaCO_3$ (ICCD: 01-086-2339) was found. The X-ray diffraction patterns obtained when examining the tablets from different angles differ in the intensity ratio of the ZnO and HA+$CaCO_3$ peaks. We assume that calcium carbonate $CaCO_3$ could be formed as a result of the interaction of hydroxyapatite and the unreacted residue of hexamethylenetetramine $C_6H_{12}N_4$ or pol-

yvinylpyrrolidone, which were used to synthesize zinc oxide by the method [28].

Figure 1 shows parts of adsorption isotherms obtained by studying the processes of nitrogen thermal desorption on the initial powders of hydroxyapatite and zinc oxide, and on one of the composites after pressing (in this example, the mixing of the initial components occurred in equal proportions). As it can be seen from Figure 1, the values of the volume of adsorbed gas recorded in the study of the composite after pressing are several times lower than those for the initial powders.

Accordingly, the registered specific surface area SBET of the composites of the entire series turned out to be expectedly lower than the specific surface area of the initial hydroxyapatite and zinc oxide used for mixing (Table 1).

Figure 2 shows a scanning electron microscopy (SEM) image of the hydroxyapatite surface before pressing (sample 1). As it can be seen from the Figure 2, the surface of the powder is represented by agglomerates about 2 μm in size, consisting of a set of nanorods. We believe that the presence of large agglomerates determines the low specific surface area shown in Table 1.

Table 1 shows that, after pressing the specific surface area of all the composites expectedly decreases, and the size of the particles in the composites in tablets increases. It should be noted that when mixing and pressing a material of lower mass, the specific surface area is 2 times higher (sample HA:ZnO (1:1)).

Table 2 presents the results of studying the specific surface area (SBET) and the dye photodegradation rate related to the specific surface area (V) of a series of zinc oxide samples synthesized for catalysis.
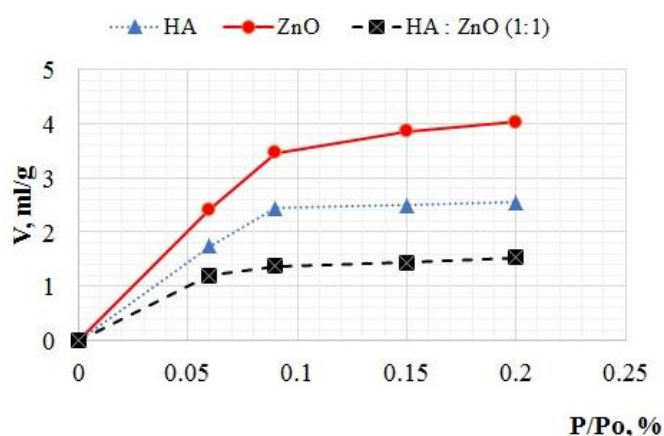
The specific surface area of pure zinc oxide, SBET, exceeds the specific surface area of the sample modified with silver nanoparticles by a factor of 3 (samples 1 and 2), but, at the same time, the dye photodegradation rate related to the specific surface area (V) for sample 1 is 3.8 times lower than that for sample 2.

For the samples obtained in the presence of SAA, the specific surface area turned out to be somewhat lower than expected, most likely due to the presence of residual molecules of sodium dodecyl sulfate on the surface. These molecules cover the surface, and the gas (N_2) cannot be adsorbed by the entire surface area, so the data are underestimated. To remove surfactants from the surface, drying was undertaken at a temperature of 250 ºC for an hour, which led to an increase in the specific surface area by 2–3 m²/g. To obtain more reliable values of the specific surface of photocatalysts synthesized in the presence of surfactants, it was necessary to anneal the powder at 250 ºC for 2–3 hours.

Analyzing the decomposition rates for the samples synthesized in the presence of SSA, we noted a positive effect of precipitated Ag NPs on the activity of the catalysts: the dye photodegradation rate for sample 5 increased by a factor of 2.75 compared to this parameter for sample 3.

It is known [4] that the intensity of the process of photocatalytic decomposition is affected by the size of the ZnO crystallite. Therefore, one of the objectives of the study was to determine the average sizes of nanoparticles in powder catalysts.
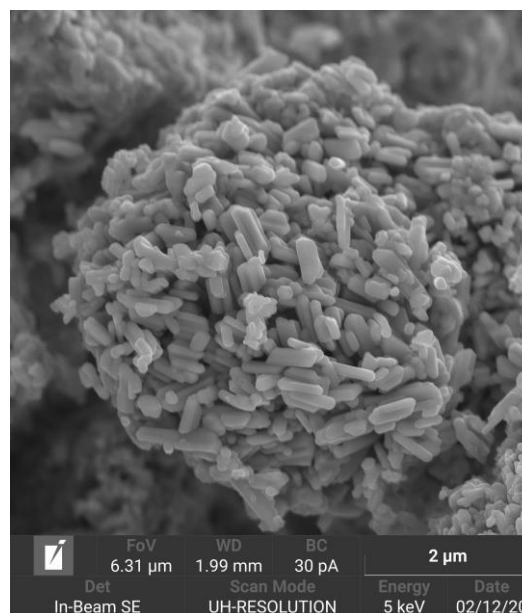

Figure 2 SEM image of the initial powder of HAP.

Figure 1 Plots of adsorption isotherms of the initial powders and the HAP:ZnO (1:1) composite.

Table 1 The specific surface area of the initial powders and the composites after pressing.

Sample	SBET, m²/g	D, nm
HA	9	191
ZnO	16	66
HA:ZnO (1:1)	5.3	258
HA:ZnO (1:3)	5.7	212
HA:ZnO (1:1)	9.9	138

Table 2 The results of the study of the specific surface area and activity of the ZnO powder catalysts.

Sample	SBET, m²/g	V, μmol/h
1	12	0.046
2	4	0.173
3	9.5	0.113
4	10	0.213
5	19	0.311

Using the specific surface area values obtained from the Sorbi device and the density of the test material, an approximate calculation of the size of the catalyst particles can be made. The average size of the particles for sample 1 is 88 nm, for sample 2 – 272 nm, for sample 3 – 107 nm, for sample 4 – 108 nm, and for sample 5 – 59 nm. Analyzing samples 4 and 5, it can be noted that the coarsening of silver nanoparticles during synthesis leads to the coarsening of ZnO aggregates.

The band gap value of a series of samples for catalysis was determined from the estimates of the absorption spectra. For pure zinc oxide it was 3.37 eV; for the sample modified only with silver – 3.33 eV. The sample synthesized with the participation of surfactants and modified with silver nanoparticles showed a band gap value of 3.35 eV.

4. Conclusions

The results of studying the specific surface area of zinc oxide modified with silver nanoparticles in the presence and absence of a surfactant made it possible to select the conditions necessary for the removal of surfactants and evaluate the efficiency of using Ag nanoparticles to increase the activity of the zinc oxide surface during catalytic decomposition.

For the composites based on zinc oxide and hydroxyapatite, sorption analysis methods made it possible to evaluate the changes that occurred in the powders after pressing in terms of nanoparticle sizes and specific surface area. According to the literature sources analysis, the considered composite structures demonstrate a high antibacterial activity and can be a promising biomaterial with improved mechanical and antibacterial properties.

It should be noted that the size estimate will be valid for cases when the particles that make up the composite are the same in size and do not have pores. If the particles in the initial powder are in the form of nanorods, the size analysis should be carried out taking into account the data on the aspect ratio of the nanorods.

Supplementary materials

Supplementary materials are available.

Funding

Acknowledgments

Author contributions

Conceptualization: E.M, V.M[1].
Data curation: N.P.
Funding acquisition: N.P, E.M, A.B.
Investigation: E.M, V.M[2], D.R.
Project administration: N.P.
Supervision: V.M[1].
Validation: A.B, N.P, A.M, V.M[2].
Writing – original draft: E.M, N.P, D.R.
Writing – review & editing: A.M, V.M[1].

Conflict of interest

The authors declare no conflict of interest.

Additional information

Author IDs:
Evgeniya Maraeva, Scopus ID 36131990800;
Anton Bobkov, Scopus ID 56898688900;
Nikita Permiakov, Scopus ID 56499046400;
Vasily Matveev, Scopus ID 57211220372;
Alexander Maximov, Scopus ID 54797495700;
Vyacheslav Moshnikov, Scopus ID 6701582758.

Websites:
Saint-Petersburg Electrotechnical University «LETI», https://etu.ru;
Petersburg Nuclear Physics Institute, http://www.pnpi.spb.ru/en.

References

1. Fang W, Yu L, Xu L. Preparation, characterization and photocatalytic performance of heterostructured CuO-ZnO-loaded composite nanofiber membranes. Beilstein J Nanotechnol. 2020;11(1):631–650. doi:10.3762/bjnano.11.50
2. Salari H, Sadeghinia M. MOF-templated synthesis of nano Ag$_2$O/ZnO/CuO heterostructure for photocatalysis. J Photochem Photobiol A. 2019;376:279–287. doi:10.1016/j.jphotochem.2019.03.010
3. Zhang QP, Li J, Xu M. Ag decorated ZnO based nanocomposites for visible light-driven photocatalytic degradation: basic understanding and outlook. J Phys D Appl Phys. 2022;55:483001. doi:10.1088/1361-6463/ac941a
4. Casey PS, Rossouw CJ, Boskovic S, Lawrence KA, Turney TW. Incorporation of dopants into the lattice of ZnO nanoparticles to control photoactivity. Superlattices Microstruct. 2006;39(1–4):97–106. doi:10.1016/j.spmi.2005.08.034
5. Ryabko AA, Nalimova SS, Mazing DS, Korepanov OA, Guketlov AM, Alexandrova OA, Maksimov AI, Moshnikov VA, Shomakhov ZV, Aleshin AN. Sensitization of zno nanorods by AgInS2 colloidal quantum dots for adsorption gas sensors with light

activation. Technical Physics. 2022;92(6):845–851. doi:10.21883/JTF.2022.06.52514.15-22

6. Zhang X, Chen YL, Liu RS. Tsai DP. Plasmonic photocatalysis. Rep Prog Phys. 2013;76:046401. doi:10.1088/0034-4885/76/4/046401

7. Sigaev AP, Averin IA, Pronin IA, Karmanov AA, Yakushova ND, Moshnikov VA. Formation peculiarities of silver dendritic structures for photocatalysts of the visible radiation range. J Phys Conf Ser. 2019;1410(1):012034. doi:10.1088/1742-6596/1410/1/012034

8. Clament Sagaya Selvam N, Vijaya JJ, Kennedy LJ. Effects of morphology and Zr doping on structural, optical, and photocatalytic properties of ZnO nanostructures. Ind Eng Chem Res. 2012;51:16333–16345. doi:10.1021/ie3016945

9. Yakushova ND, Averin IA, Donkova BV, Dimitrov DT, Pronin IA, Mazing DS, Aleksandrova OA, Moshnikov VA. Photocatalytic and photoluminescence properties of the copper and manganese modified zinc oxide. In: Proceedings of the 2016 IEEE North West Russia Section Young Researchers in Electrical and Electronic Engineering Conference; 2016 Feb 2–3; Saint-Petersburg, Russia. p. 105. doi:10.1109/EIConRusNW.2016.7448131

10. Karpova SS, Moshnikov VA, Mjakin SV, Kolovangina ES. Surface functional composition and sensor properties of ZnO, Fe_2O_3, and $ZnFe_2O_4$. Semiconduct. 2013;47(3);392–395. doi:10.1134/S1063782613030123

11. Sigaev AP, Averin IA, Karmanov AA, Pronin IA, Yakushova ND. Investigation of the effect of plasma treatment on the concentration of adsorption centers on the surface of nanostructured materials based on SiO_2-SnO_2. In: Proceedings of the International Symposium "Reliability and Quality"; 2020 May 25–31; Penza, Russia. p. 257.

12. Pronin IA, Yakushova ND, Averin IA, Karmanov AA, Komolov AS, Sychev MM, Moshnikov VA, Terukov EI. Chemical binding of carbon dioxide on zinc oxide powders prepared by mechanical milling. Inorg Mater. 2021;57(11):1140–1144. doi:10.1134/S0020168521110108

13. Pronin IA, Yakushova ND, Sychev MM, Komolov AS, Myakin SV, Karmanov AA, Averin IA, Moshnikov VA. Evolution of acid–base properties of the surface of zinc oxide powders obtained by the method of grinding in an attritor. Glass Phys Chem. 2018;44(5):464–473. doi:10.1134/S1087659618050140

14. Levkevich EA, Moshnikov VA, Maximov AI, Yukhnovets OB. Photocatalytic properties of ZnO/CuO heterostructures. In: Proceedings of the 2019 IEEE North West Russia Section Young Researchers in Electrical and Electronic Engineering Conference; 2019 Jan 28–30; Saint-Petersburg, Russia. p. 777. doi:10.1109/EIConRus.2019.8657316

15. Hoai PTT, Huong NTM, Huong PT, Viet NM. Improved the light adsorption and separation of charge carriers to boost photocatalytic conversion of CO_2 by using silver doped ZnO photocatalyst. Catalysts. 2022;12:1194. doi:10.3390/catal12101194

16. Radičić R, Maletić D, Blažeka D, Car J, Krstulović N. Synthesis of silver, gold, and platinum doped zinc oxide nanoparticles by pulsed laser ablation in water. Nanomater. 2022;12(19):3484. doi:10.3390/nano12193484

17. Liu X, Li W, Chen N, Xing X, Dong C, Wang Y. Ag-ZnO heterostructure nanoparticles with plasmon-enhanced catalytic

degradation for Congo red under visible light. RSC Adv. 2015;5:34456–34465. doi:10.1039/C5RA03143E

18. Shelemanov AA, Evstropiev SK, Karavaeva AV, Nikonorov NV, Vasilyev VN, Podruhin YF, Kiselev VM. Enhanced singlet oxygen photogeneration by bactericidal ZnO–MgO–Ag nanocomposites. Mater Chem Phys. 2022;276:125204. doi:10.1016/j.matchemphys.2021.125204

19. Al Rugaie O, Jabir MS, Mohammed MK, Abbas RH, Ahmed DS, Sulaiman GM, Mohammed SAA, Khan RA, Al-Regaiey KA, Al-sharidah M, Mohany KM, Mohammed HA. Modification of SWCNTs with hybrid materials ZnO–Ag and ZnO–Au for enhancing bactericidal activity of phagocytic cells against Escherichia coli through NOX2 pathway. Sci Rep. 2022;12(1):17203. doi:10.1038/s41598-022-22193-1

20. Turlybekuly A, Pogrebnjak AD, Sukhodub LF, Suhodub LB, Kistaubayeva AS, Savitskaya IS, Shokatayeva DH, Bondar OV, Shaimardanov ZhK, Plotnikov SV, Shaimardanova BH, Digel, I. Synthesis, characterization, in vitro biocompatibility and antibacterial properties study of nanocomposite materials based on hydroxyapatite-biphasic ZnO micro- and nanoparticles embedded in Alginate matrix. Mater Sci Eng C. 2019;104:109965. doi:10.1016/j.msec.2019.109965

21. Shitole AA, Raut PW, Sharma N, Giram P, Khandwekar AP, Garnaik B. Electrospun polycaprolactone/hydroxyapatite/ZnO nanofibers as potential biomaterials for bone tissue regeneration. J Mater Sci Mater Med. 2019;30(5):51. doi:10.1007/s10856-019-6255-5

22. Cheng K, Guan Z, Weng W, Wang H, Lin J, Du P, Han G. Hydroxyapatite/ZnO-nanorod composite coatings with adjustable hydrophilicity and Zn release ability. Thin Solid Films. 2013;544:260–264. doi:10.1016/j.tsf.2013.03.108

23. Behnamsani A, Meshkini A. Synthesis and engineering of mesoporous ZnO@HAP heterostructure as a pH-sensitive nano-photosensitizer for chemo-photodynamic therapy of malignant tumor cells. J Drug Deliv Sci Technol. 2019;53:101200. doi:10.1016/j.jddst.2019.101200

24. Sarwar S, Chakraborti S, Bera S, Sheikh IA, Hoque KM, Chakrabarti P. The antimicrobial activity of ZnO nanoparticles against Vibrio cholerae: Variation in response depends on biotype. Nanomed Nanotechnol Biol Med. 2016;12(6):1499–1509. doi:10.1016/j.nano.2016.02.006

25. Saxena V, Hasan A, Pandey LM. Effect of Zn/ZnO integration with hydroxyapatite: a review. Mater Technol. 2018;33(2):79–92. doi:10.1080/10667857.2017.1377972

26. Maraeva EV, Permiakov NV, Kedruk YY, Gritsenko LV, Abdullin KA. Creating a virtual device for processing the results of sorption measurements in the study of zinc oxide nanorods. Chim Techno Acta. 2020;7(4):154–158. doi:10.15826/chimtech.2020.7.4.03

27. Khalugarova KN, Maraeva EV, Zaikina AV., Matveev VA., Moshnikov VA. Influence of heating time and microwave radiation power on the microstructure and phase composition of calcium-phosphorus compounds during formation. J Phys Conf Ser. 2020;1697(1):012050. doi:10.1088/1742-6596/1697/1/012050

28. Yukhnovets O, Semenova AA, Levkevich EA, Maximov AI, Moshnikov VA. J Phys Conf Ser. 2018;993(1):012009. doi:10.1088/1742-6596/993/1/012009